A dual functional NBD chemosensor for the colorimetric and fluorimetric detection of fluoride

B. Vidya[1], R. V. Sumesh[2]
[1,2]*Assistant Professor, Dept. of Chemistry, Sree Narayana College, Alathur*

***Abstract*—An NBD based dual functional chemosensor (2-hydroxy *N′* (7-nitrobenzo [1,2,5] oxadiazol 4 yl) benzo hydrazide (NBD-SH) has been designed using hydrazide platform. Exploiting well known stokes shift of NBD and absorption in visible region, a new radiometric fluorescent chemosensor capable of visibly detecting fluoride has been synthesized. Upon addition of fluoride ion, the probe displays apparent colour change from yellow to wine red. The probe exhibits high selectivity for fluoride with respect to other common anions. In addition, the probe has been successively utilized for detection of fluoride *via* test dots.**

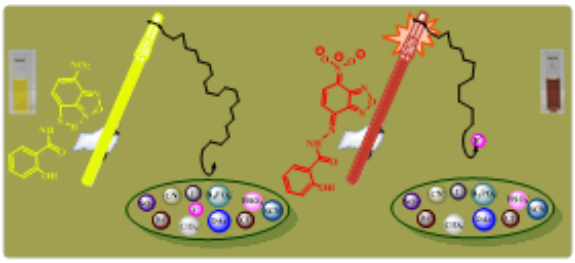

***Index Terms*—NBD-SH, ratio metric, chemosensor, F^-.**

I. INTRODUCTION

Anions are essential to life as many biological processes depend on the presence or transport of anions, or use anion to carry out chemical transformations [1]. Henceforth the development of new receptors, sensors and transporters for anionic species continues to be an upsurge of interest [2]. Unique property of fluoride compared to its congeners as a result of relative size, high electron density and largest electro negativity make an attractive target to the scientific community. As the role of fluoride in the treatment of osteoporosis [3], dental care [4], food processing are exposed, the detrimental effects are associated with increased concentration leading to dramatic side effects such as osteosarcoma [5], gastric and kidney disorders, dental and skeletal fluorosis, urolithiasis in humans and even death [6]. With regard to chemical sciences, the focus on fluoride from other anion is attributed due to its emphasis in agriculture, associated with nerve gases and refinement of uranium used in nuclear weapons manufacture etc. is noteworthy. Because of these successive advantages and harmful effects of fluoride ions, developing a method to monitor fluoride ions has fascinated many researchers. Traditional methods such as the Willard Winter and Ion chromatography require costlier instrumentation and tedious procedure [7]. Whereas the two detection methods such as colorimetry and fluorimetry opted in chemosensor chemistry are mostly advantageous due to the simplicity, high sensitivity, ready availability, low cost, and their applicability in living cells (*in vivo*) for the detection of fluoride. In addition, colorimetric methods are far easy to implement in practical applications (test stripes/dips sticks).

Henceforth designing a chemosensor operating *via* dual method is the target. In an effort to address these issues, we moved forward to design a new fluoride detecting system based on NBD salicylhydrazide (NBD-SH). Hydrazides have been extensively used in several research fields owing to their facile synthesis, tune able electronic properties, and good chelating capability [8]. Recently M. Sukwattanasinitt et al. [9] reported a series of bishydrazide compounds for selective detection of aluminium in aqueous solution which displayed large Stoke's shift up to 133 nm and emission colours varying from blue to orange. On the other hand, NBD has been used as a chromophore because NBD has high extinction coefficient, high quantum yield, high chemical stability, and ability to display visible ICT absorption band with large Stoke's shift,[10] although their aromatic plane is smaller

[11]-[21]. A large Stoke's shift is also beneficial in fluorescence sensing technology to avoid self-absorption and interference from light source. Probes with emission in the near IR region are optimal for biological applications due to minimal photo damage to biological samples and minimum interference from background auto-fluorescence in living systems. Therefore, it is highly desirable in bioimaging to develop new types of probes that has ability in optical tuning toward near IR region.

II. RESULT AND DISCUSSION

The chemosensor was synthesized with ease by treating salicylhydrazide in ethanol with 4-chloro-7-nitrobenzo [1,2,5] oxadiazole (NBD) solution (Scheme 2.1). The probe NBD-SH was well characterized by ^{1}H, ^{13}C NMR spectroscopy and ESI–MS. In the design of fluorescent chemosensor 2-hydroxy-*N'*-(7-nitrobenzo [1,2,5] oxadiazol-4-yl) benzo hydrazide (NBD-SH), the NBD framework has been chosen as it possesses larger Stoke's shift and visible absorption band due to the ICT effect even though it possesses a smaller aromatic plane. Herein we report the structural characterization and photonic studies on the novel fluorescent probe NBD-SH that reveals its efficiency as selective chemosensor for F^- detection in HEPES buffered solution (10% CH_3CN as co solvent) at pH = 7.4 (10 mM) medium.

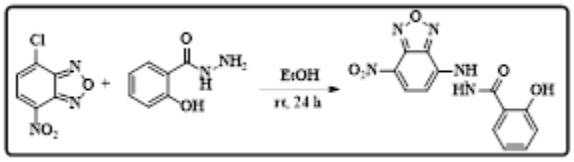

Scheme 2.1: Synthesis of probe 2-hydroxy-*N'* (7-nitrobenzo [1,2,5] oxadiazol-4-yl) benzohydrazide (NBD-SH).

Upon adding fluoride, the colour changed from yellow to wine red probably by virtue of its strong affinity for F^- (Figure 2.1). This intern indicates that probe can act as a new visual sensor for F^-. Notably addition of other anions to NBD-SH exerted no changes in the colour. The excellent selectivity of NBD-SH for F^- over other anions is evident from the pronounced differences in absorbance and colour changes.

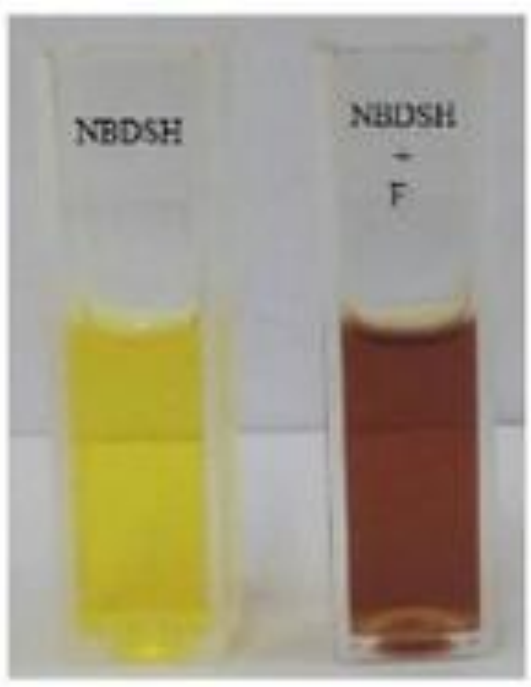

Figure 2.1. Colour change of probe NBD-SH in the presence of F^-.

The UV-visible absorption properties of NBD-SH were investigated by UV-visible absorption spectrum with salts containing anions such as F^-, Cl^-, Br^-, I^-, CN^-, OAc^-, NO_3^-, ClO_4^-, HSO_4^-, $H_2PO_4^-$ and SCN^- in HEPES buffered solution (10% CH_3CN as co solvent) at pH = 7.4 (10 mM). The probe exhibited a characteristic absorption band at 338 nm and another small band at 501 nm. While addition of other anions did not induce any discernible changes (Figure 2.2a), presence of F^- ion induced the appearance of two new absorption bands at 466 nm and 711 nm in absorption profile. It is worth noting that a band observed at about 338 nm experienced a red shift to 358 nm (Figure 2.2a).

To study the sensitivity of the probe, NBD-SH was titrated with fluoride ion up to 10 equivalents. When increasing the concentration of F^- a new absorption band at 466 nm gradually emerged while the intensity of absorption band at 338 nm decreased with a 20 nm red shift, and a new band at 711 nm increased simultaneously. Two isosbestic points observed at 348 and 556 nm throughout the titration indicate the formation of new species by the influence of F^- with NBD-SH (Figure 2.2b). The appearance of a new peak close to the near IR region is certainly advantageous

for their applications in biological systems. All these result shows that probe NBD-SH has good selectivity and high sensitivity for F^- over the competitive anions.

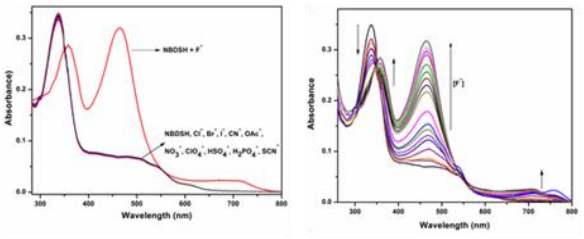

Figure 2.2. (a) UV-visible spectral changes of NBD-SH (10 μM) upon addition of various anions (5 equiv.); (b) incremental addition of F^- (10 equiv.) in HEPES buffered solution (10% CH_3CN as co solvent) at pH = 7.4 (10 mM).

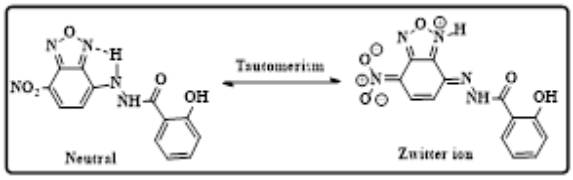

Scheme 2.2. Intramolecular hydrogen bonding.

Eventually the anion binding affinities and fluoro responses of the probe in HEPES buffer were studied by fluorescence spectroscopy. The fluorescence spectra of NBD-SH in HEPES buffered solution (10% CH_3CN as co solvent) at pH = 7.4 (10 mM) exhibited emission bands at 568 nm and 480 nm (shoulder) when excited at 400 nm. A larger Stoke's shift value (approx. 250 nm) suggests significant structural changes between the ground and excited states upon photoexcitation. Indeed, both above parameters suggest the possibility of intramolecular proton transfer processes. The reduced electron density at the amino nitrogen in the LUMO+1 weakens the NH bond, making the proton dissociation more facile, while the relatively higher electron density at the oxadiazol/furazan nitrogen attracts the proton. This forms a strain-free, five membered rings including the hydrogen bond, an ideal factor that facilitates the proton transfer processes (Scheme 2.2). The fluorescent spectrum of probe NBD-SH was investigated in the presence of various anions like Cl^-, Br^-, I^-, CN^-, OAc^-, NO_3^-, ClO_4^-, HSO_4^-, $H_2PO_4^-$ and SCN^- (Figure 2.3a). No detectable fluorescence changes were observed when five equiv. of these anions was added individually to NBD-SH. However, addition of F^- quenches the fluorescence at 480 nm with a dramatic, progressive enhancement of red shifted band at 610 nm. The fluoride induced deprotonation induces the disappearance of normal and tautomer fluorescence and favors the new emission from the deprotonated state. Thus, the sensing mechanism in this case would be the inhibition of ESIPT process. A ratio metric fluorescence response can be derived by plotting the intensities at two different wavelengths 610/480 nm. This clearly opines that the receptor NBD-SH is a selective sensor for F^-.

To further evaluate the responsive nature of probe towards F^-, fluorescence titration with F^- by varying concentration was studied. As shown in Figure 2.3b, on increasing concentration of F^-, a gradual increase in fluorescent intensity was observed. The band at 568 nm underwent a bathochromic shift of 42 nm and reached a maximum at 610 nm upon titrating NBD-SH with aliquot addition of F^- ion. The sensing mechanism of NBD-SH for F^- anions could be attributed to the interaction between the F^- with the amino proton of NBD-SH through hydrogen bonding interactions. The N-H proton becomes more acidic as it is intramolecularly hydrogen bonded to furazan nitrogen of NBD moiety bearing a strongly electron withdrawing nitro group, and hence the addition of excess F^- would lead to the deprotonation of the N-H proton.

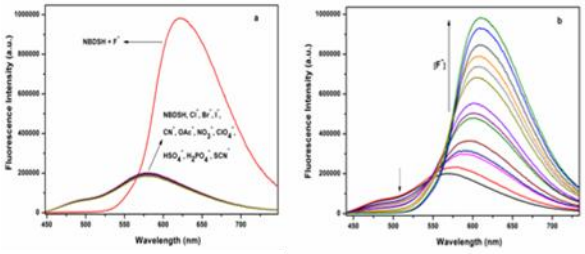

Figure 2.3. (a) Fluorescence intensity of NBD-SH (10 μM) upon addition of various anions (5 equiv.); (b) incremental addition of F^- (10 equiv.) in HEPES buffered solution (10% CH_3CN as co solvent) at pH = 7.4 (10 mM).

The binding of F^- with NBD-SH was confirmed as 1:1 stoichiometry by Job's plot method (Figure 2.4a). From the fluorescence titration profile, the detection

limit was found to be 5.32 x 10^{-8} M (Figure 2.4b) [22]. The binding constant was calculated to be 5.70 x 10^{6} M^{-1}[23].

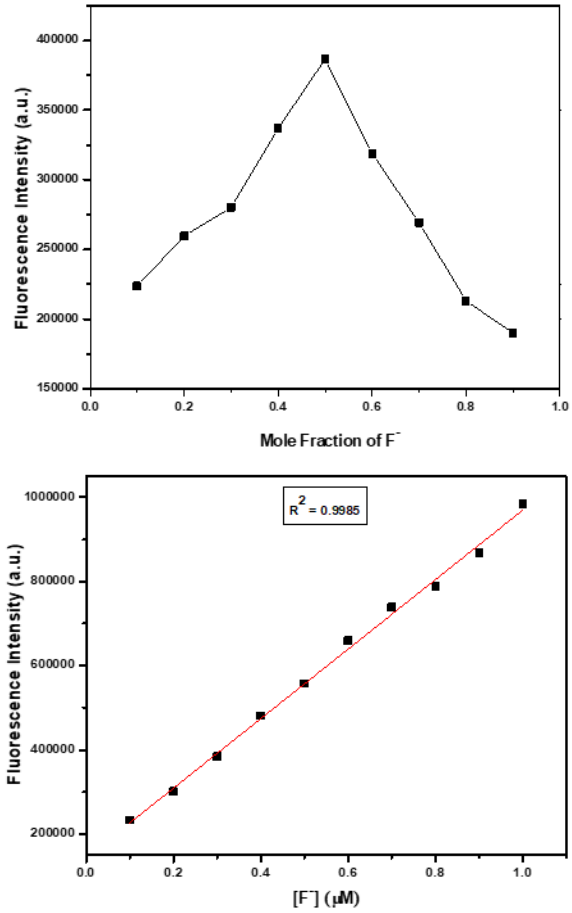

Figure 2.4. (a) Job's plot of NBD-SH and F^-, which indicated the stoichiometry of 1:1 complex; (b) Plot of fluorescence intensity of NBD-SH *vs* concentration of F^-.

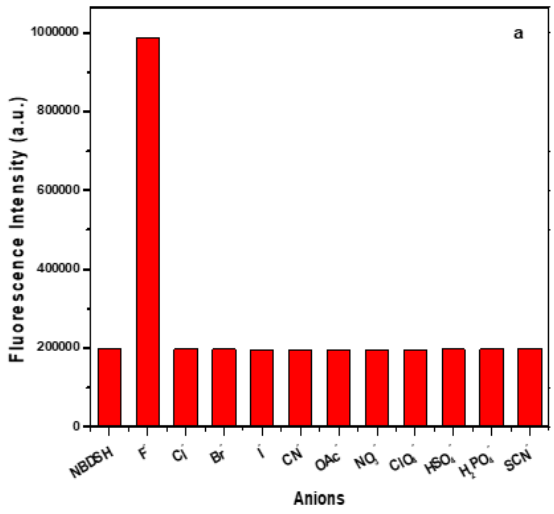

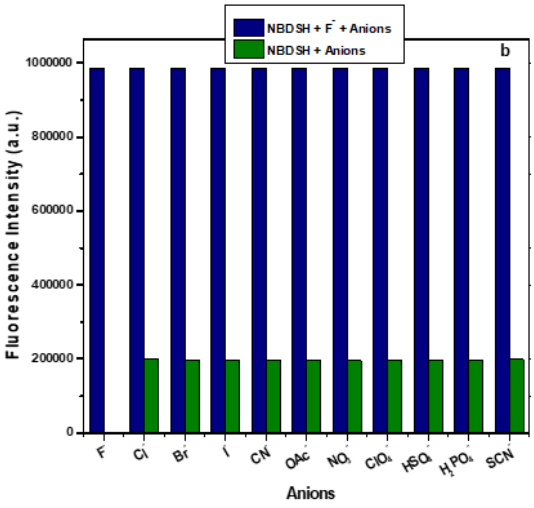

Figure 2.5. (a) Selectivty and (b) competitive fluorescence response of NBD-SH to F^- λ_{ex} at 400 nm in the presence of other analytes.

^{1}H NMR titration of the probe with tetrabutyl ammonium fluoride in $CDCl_3$ clearly shows (Figure 2.6) the participation of amino NH protons in fluoride binding. The NH proton resonance at 11.0 ppm is getting broad, shifted and eventually disappeared after subsequent addition of TBAF. This indicates that F^- interacts with NBD-SH through hydrogen bonding interactions followed by deprotonation of NH proton.

The interference of various anions if any was monitored in the presence of F^-(10 μM) with the addition of other anions such as (Cl^-, Br^-, I^-, CN^-, OAc, NO_3^-, ClO_4^- HSO_4^-, $H_2PO_4^-$ and SCN^-) (100 μM). The results show no significant changes in the fluorescence enhancement in comparison with that observed in the presence of F^- alone. This reveals that probe has good selectivity towards F^- over other anions (Figure 2.5).

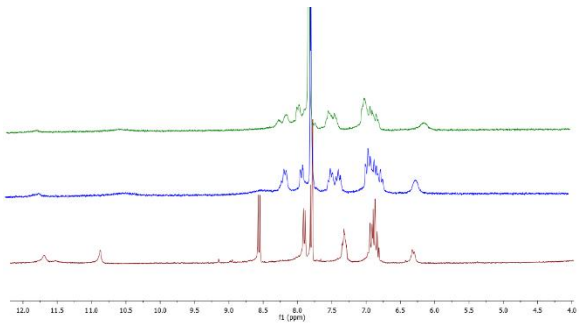

Figure 2.6. ^{1}H NMR spectral changes of NBD-SH upon addition of F^- in $CDCl_3$.

After deprotonation the lone pair of electrons present on the nitrogen atom may migrate as shown in the Scheme 2.3 and thereby attain conjugation extended planar geometry which could be seen from the optimized geometry of the deprotonated species (Figure 2.7).

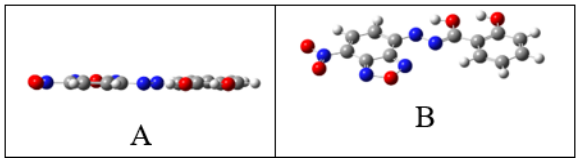

Figure 2.7. Optimized geometries of NBD-SH after deprotonation; (a) side view; (b) normal view.

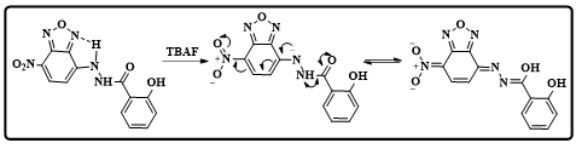

Scheme 2.3. Delocalization of probe after deprotonation.

The geometries of the sensor NBD-SH and F^- bound NBD-SH were optimized using DFT-B3LYP levels using Gaussian 03 package [24]. The optimized geometries of the probe and its 1:1 complex with F^- are shown in Figure 2.8, in which the effective binding sites, namely NH for F^- is displayed. The bond length of N-H i.e. hydrogen bonded to nitrogen of furazan ring is found to be 2.541 Å in the probe NBD-SH. Hence, the increase in distance between nitrogen of furazan ring and N-H proton indicates the least feasible nature of hydrogen bonding. Moreover, the optimized structure of fluoride appended probe NBD-SH shows that the bond length of N-H is increased to 1.029 Å from 1.015 Å in the probe. It is well clear that the binding of fluoride leads to the increase in the bond length of the N–H bond. Obviously, the bond length of O-H bond remains same. To get an insight into the electronic behaviour in the presence and absence of F^- with NBD-SH, TD-DFT calculations were carried out using the same level. The calculated HOMO–LUMO energy gaps of NBD-SH and NBD-SH + F^- are 3.3218 eV and 1.9466 eV, respectively. There is a considerable difference in the energy minimization structure in NBD-SH and the NBD-SH + F^- adduct, which can shed light on the changes in the absorption spectra and the corresponding changes in colour. In the optimized structure of NBD-SH, the salicylyl group adopted a tilted geometry with the NBD group. While the optimized geometry of NBD-SH after deprotonation clearly shows total planarity (Figure 2.7). This structural difference gives rise to the difference in π-conjugation between probe and deprotonated form and hence the operation of ICT. So, the shift in fluorescence towards the red region mainly due to charge transfer from salicycyl to nitro group of NBD.

The well separated distribution between HOMO and LUMO upon F^- binding indicates hydrogen bonding when the molecule is excited (Figure 2.9).

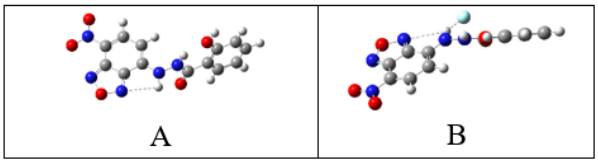

Figure 2.8. Optimized geometries of (a) NBD-SH and (b) its 1:1 complex with F^-.

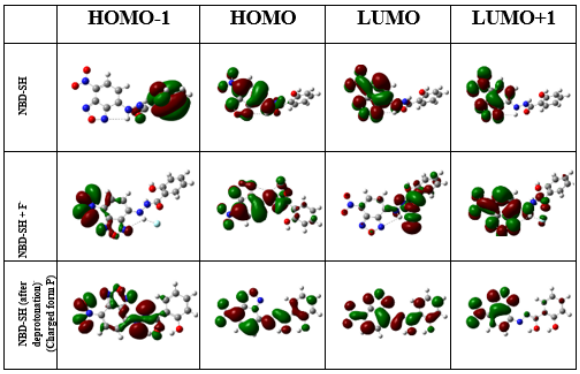

Figure 2.9. Frontier molecular orbitals of NBD-SH and NBD-SH + F^- obtained from the DFT calculations using Gaussian 03 program.

The positive response of NBD-SH toward F^- has encouraged us to develop a test kit for the practical application of the sensor. Test strips were prepared by immersing filter papers into an aqueous solution of NBD-SH and then drying in air. After dropping the aqueous solutions of various anions (Cl^-, Br^-, I^-, F^-, CN^-, OAc^-, NO_3^-, ClO_4^-, HSO_4^-, $H_2PO_4^-$ and SCN^-), only the F^- ion shows the obvious colour change from yellow to wine red (Figure 2.10). Therefore, the test strips could directly detect the anions in aqueous solution, which demonstrates the high sensitivity of the sensor NBD-SH in solid state.

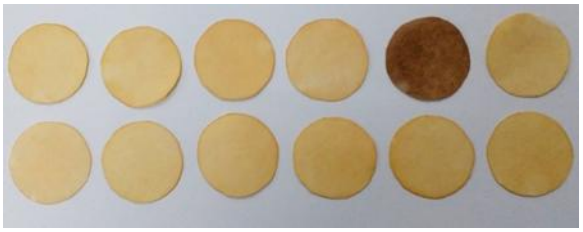

Figure 2.10. Photographs of NBD-SH based test strips for colorimetric detection of F^-; Left to right: NBD-SH, Cl^-, Br^-, I^-, F^- and CN^- (Top), OAc^-, NO_3^-, ClO_4^-, HSO_4^-, $H_2PO_4^-$ and SCN^- (Bottom).

III. CONCLUSION

In summary, we have synthesised NBD-salicylhydrazide conjugate and utilised as sensor for fluoride ions. The probe exhibited very high selectivity and sensitivity for the colorimetric and fluorimetric detection of fluoride ion with the detection limit value of 5.32 x 10^{-8} M, respectively. The change in UV-visible absorption and Fluorescence spectral features with appropriate colour change of NBD-SH in presence of F^- is due to fluoride ion induced deprotonation of NBD-SH, respectively which were further supported by mass spectrometry and ^1H NMR titrations. Test dots of NBD-SH provide a convenient way to sense this toxic anion.

Supporting information: synthetic, experimental procedures and spectra are available in supporting information.

IV. ACKNOWLEDGEMENT

BV and SRV acknowledge DST-IRHPA, FIST and PURSE, MKU, Tamilnadu, for instrumental facilities.

REFERENCE

[1] Bianchi, K. J. Bowman, and E. E. Gracia, Supramolecular Chemistry of Anions. New York, NY, USA: Wiley-VCH, 1997.
[2] P. A. Gale and S. E. Garcia-Garrido, "Anion receptors," J. Chem. Soc. Rev., vol. 37, pp. 151–190, 2008.
[3] P. A. Gale and R. Quesada, "Anion coordination and separation," Coord. Chem. Rev., vol. 250, pp. 3219–3244, 2006.
[4] J. L. Sessler, P. A. Gale, and W. S. Cho, Anion Receptor Chemistry. Cambridge, UK: Royal Society of Chemistry, 2006.
[5] K. B. James and E. G. Espana, "Supramolecular chemistry of anions," in Supramolecular Chemistry of Anions, A. Bianchi, Ed. New York, NY, USA: Wiley-VCH, 1997.
[6] D. Briancon, "Treatment of bone diseases," Rev. Rheum., vol. 64, p. 78, 1997.
[7] S. Matuso, K. Kiyomiya, and M. Kurebe, "Toxicity studies," Arch. Toxicol., vol. 72, p. 798, 1998.
[8] E. B. Bassin, D. Wypij, R. B. Davis, and M. A. Mittleman, "Age-specific fluoride exposure," Cancer Causes Control, vol. 17, p. 421, 2006.
[9] P. P. Singh et al., "Urolithiasis and fluoride," Urol. Res., vol. 29, p. 238, 2001.
[10] B. L. Riggs, Bone and Mineral Research, Annual 2. Amsterdam, Netherlands: Elsevier, 1984.
[11] M. Kleerekoper, "Fluoride and the skeleton," Endocrinol. Metab. Clin. North Am., vol. 27, p. 441, 1998.
[12] M. A. G. T. van den Hoop, R. F. M. J. Cleven, J. J. Van Staden, and J. Neele, "Anion analysis," J. Chromatogr. A, vol. 739, p. 241, 1996.
[13] M. C. Breadmore et al., "Capillary electrophoresis of inorganic anions," Anal. Chem., vol. 74, p. 2112, 2002.
[14] B. N. Raj and M. R. P. Kurup, "Spectroscopic studies," Spectrochim. Acta A, vol. 66, p. 898, 2007.
[15] K. Boonkitpatarakul et al., "Fluorescent sensors," ACS Sens., vol. 1, p. 144, 2016.
[16] R. E. Pagano and R. G. Sleight, "Defining lipid transport," Science, vol. 229, p. 1051, 1985.
[17] J. H. Kim, J. Y. Noh, I. H. Hwang, J. J. Lee, and C. Kim, "Fluoride sensing," Tetrahedron Lett., vol. 30, p. 4001, 2013.
[18] J. Tan and X. Yan, "Nano-sensors," Talanta, vol. 1, p. 9, 2008.
[19] S. Liu and S. Wu, "Fluorescence sensing of anions," J. Fluoresc., vol. 4, p. 1599, 2011.
[20] F. Qian et al., "Zinc sensors," J. Am. Chem. Soc., vol. 4, p. 1460, 2009.
[21] Z. Xie et al., "New fluorescent receptors," New J. Chem., vol. 3, p. 607, 2011.
[22] Z. Xu et al., "Anion recognition," Tetrahedron, vol. 65, p. 2307, 2009.

[23] Y. B. Ruan, S. Maisonneuve, and J. Xie, "Colorimetric sensing," Dyes Pigm., vol. 90, p. 239, 2011.
[24] K. Liu, Y. Zhou, and C. Yao, "Anion sensor design," Inorg. Chem. Commun., vol. 14, p. 1798, 2011.
[25] N. Wanichacheva, M. Siriprumpoonthum, A. Kamkaew, and K. Grudpan, "Chemosensors," Tetrahedron Lett., vol. 50, p. 1783, 2009.
[26] Z. Wang, M. A. Palacios, G. Zyryanov, and P. Anzebacher, "Sensor arrays," Chem. Eur. J., vol. 14, p. 8540, 2008.
[27] Y. Fu et al., "Calixarene-based sensors," Sens. Actuators B, vol. 164, p. 69, 2012.
[28] M. Shortreed, R. Kopelman, M. Kuhn, and B. Hoyland, "Fiber-optic sensors," Anal. Chem., vol. 68, p. 1414, 1996.
[29] K. A. Conners, Binding Constants: The Determination of Molecular Complex Stability. New York, NY, USA: Wiley, 1987.
[30] M. J. Frisch et al., Gaussian 03, Revision C.02. Wallingford, CT, USA: Gaussian, Inc., 2004.